Polymer Chemistry

REVIEW

Honeycomb structured polymer films *via* breath figures

Maribel Hernández-Guerrero*[a] and Martina H. Stenzel[b]

Among various structuring techniques, a water-driven 'templating' method for the fabrication of highly ordered porous membranes has been widely exploited for the past 17 years due to its versatility and robustness. This simple method relies on the formation of "breath figures" and the assembly of a polymer around them, resulting in the production of membranes with hexagonally arranged pores known as honeycomb structured porous polymer films/membranes. Herein, we present a review of relevant literature to stress on the advantages of this simple templating method compared with the wide range of conventional templating and lithographic techniques that have been previously used in the field. Furthermore, we present a comprehensive review on the progress in the field including the study of relevant variables, the materials that have been used, the combination of the method with other techniques, some current and potential applications for the membranes as well as characterization techniques.

Introduction

Although inconvenient in some areas such as heat exchange, coatings, paints, or even in everyday life, the formation of "breath figures" derived from condensation is the key for templating highly ordered porous polymeric membranes.

This review focuses on a novel and versatile "breath figures" templating technique. It presents the development, progress, the advantages, shortcomings, applications and future directions of the technique.

Over the past 16 years "breath figures", together with the self-assembly of a wide range of polymeric materials, have been used as an alternative method to the conventional templating and lithographic techniques for structuring micro- and nano-materials.

Compared to traditional structuring of materials, the versatility of the technique resides in the use of water condensates as dynamic templates with no fixed size. Therefore, and in contrast to other techniques, the need for fabrication of specially designed templates or very specialized machinery to fabricate them is avoided. The spontaneous evaporation of the templates "water" saves an additional calcination or selective dissolution process. In addition, variable tuning during membrane formation allows for control of the membrane properties.

[a]*Departamento de Procesos y Tecnología, División de Ciencias Naturales e Ingeniería, Universidad Autónoma Metropolitana-Cuajimalpa, Artificios 40 Colonia Miguel Hidalgo. Delegación Álvaro Obregón, México, D.F., México. E-mail: mhernandez@correo.cua.uam.mx; Fax: +52 55 26 36 38 00 3832; Tel: +52 55 26 36 38 00 3818*
[b]*The Centre for Advanced Macromolecular Design, School of Chemical Engineering and Industrial Chemistry, The University of New South Wales, Sydney, New South Wales, 2052, Australia. E-mail: mstenzel@unsw.edu.au; Fax: +61 2 9385 6250; Tel: +61 2 9385 4344*

Rapidly developed, this technique has been exploited to obtain mono- or multi-layered polymeric membranes of various pore sizes by tuning variables including humidity, concentration, polymer type, polymer architecture and molecular weight, among others. However, despite the proven simplicity and versatility of the method, a thorough insight into the key steps governing the complex mechanism of formation of the membranes is still probably the major shortcoming of the area. A full understanding of the process of formation of the porous membranes will result in a better control of the pore size, the pore size distribution and the membrane properties and will ultimately allow for the implementation of the technique at the industrial scale.

Some works have already used bare and functionalized honeycomb membranes for biotechnological applications, while other applications have been suggested. However, a finer tuning of the membrane properties and industrialization could lead to a vast range of potential and promising applications in relevant areas such as engineering, biotechnology and opto-electronics, among others.

Development of the technique

From breath figures to honeycomb structured membranes

"Breath figures" were studied as early as 1911 by Lord Rayleigh who noticed the formation of organized arrays of lens-shaped water droplets on clean surfaces.[1] The spontaneously condensed droplets were stable at the beginning of the process, grew over time and finally coalesced, giving rise to bigger and disordered water droplets. Further studies on condensation identified the steps of the formation of "breath figures" and coverage in various surfaces.[2,3] These steps include nucleation,[4,5] further

condensation and growth until the droplets reach a critical size and coalesce with neighbouring droplets. In this manner, the order of the initial droplet array is lost.

Based on this formation of "breath figures", the natural condensation that occurs on surfaces that are subjected to a highly humid environment is nowadays exploited as a templating method. Highly ordered porous films (also called honeycomb structured porous membranes, due to their hexagonal pattern) are obtained when drop-casting a polymer solution under a humid environment of at least 50% RH. In this technique, as in the phenomenon observed by Rayleigh, nucleation and growth of water droplets occur. However, in this particular "breath figures" templating technique, coalescence of water droplets is prevented by the presence of the polymer that assembles around the droplets acting like a stabilizer.

The first work on "breath figures" templating to obtain porous membranes dates from 1994. François and co-workers obtained polystyrene (PS) based honeycomb membranes from solvent casting CS_2-polymer solutions (2–100 g L^{-1}) under a humid environment.[6] Ever since this first report, the technique has been used extensively due to its versatility compared with other techniques that are briefly described below.

Traditional templating and breath figure templating

The patterning of nano- and micro-porous materials is a topic of extensive research and of applicability in medicine, pharmaceutics, biotechnology, catalysis, optics, electronics, industry and manufacturing.[7–9] Therefore, a growing number of studies focus on finding viable means for their production.

Conventionally, 'top-down', 'bottom-up', or hybrid techniques are used to pattern materials.[10] These approaches include traditional methods such as etching, lithography, photolithography and soft lithography.[11–14] Moreover, templating methods have been also explored widely. These methods use inorganic particles,[15] beads,[16] latex spheres,[17] water in-oil-emulsions,[14] bacteria,[18,19] phase separated block copolymers,[20,21] colloidal crystals,[22–24] rod-coil polymers,[25,26] and even ice crystals[27] as templates.

An alternative and more versatile method to structure materials, in particular to obtain porous membranes with a hexagonal array, is the "breath figures" templating technique. This technique, based on non-rigid templates (i.e. water droplets), allows for an interactive control and tuning of the pore size, pore spacing and final properties of the membranes such as controlled hydrophobicity or functionality. Materials with pores in the nano- or micro-scales are obtained with this technique by simply modifying the conditions during membrane fabrication.[28]

The breath figure method to produce honeycomb structured porous membranes

As first applied by François and co-workers, the method to produce honeycomb structured porous polymer films via "breath figures" (Fig. 1) consists in simply drop-casting a small volume of a polymer solution onto a solid substrate under a highly humid environment (generally at least 50% RH).

The generally accepted mechanism behind the formation of honeycomb films involves: (1) a cold surface created by the
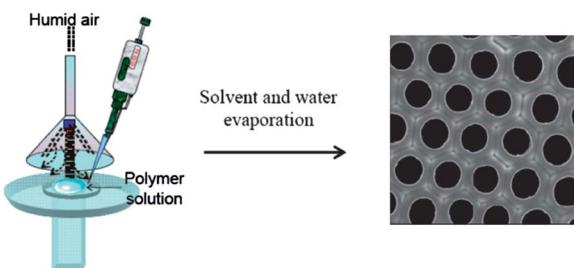
Fig. 1 Basic "breath figures" casting technique for the formation of honeycomb structured porous polymer membranes (left). Microscopy image of a typical honeycomb structured porous film (right).

evaporating solvent of the polymer solution, (2) water condensation on the solution, (3) movement and arrangement of the condensed water droplets into organized islands with hexagonal packing, (4) stabilization of water droplets through polymer precipitation (polymer envelope around the droplets)—in this way, the condensed water droplets serve as molds for the pores, (5) total evaporation of the casting solvent followed by a pressure increase leading to the bursting of the polymer envelope to form pores and (6) finally, total evaporation of water to reveal a porous film (see Fig. 2).

After evaporation is completed, the opaque polymeric films that remain attached to the solid substrate are porous. In contrast, when casting under dry conditions the films are transparent and devoid of pores. Variations to the basic technique have also rendered highly regular porous polymeric membranes (see Fig. 3). These variations rely on the control of some variables such as airflow rate, type of substrate and temperature. Some of these variations and combinations of the technique with other methods are presented as follows.

Airflow technique. As in the basic technique, the polymer solution is cast onto a solid substrate. However, the forced and rapid solvent evaporation caused by an air current creates a bigger temperature gradient between the surface of the polymer solution and the bulk.[29–33] A colder surface promotes the condensation and growth of the water droplets. In addition, close packing is favoured due to the currents and movement in the
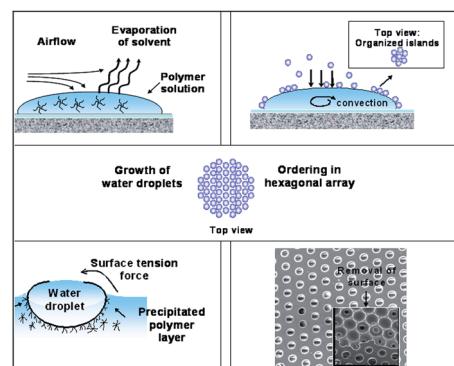

Fig. 2 Mechanism of formation of honeycomb structured porous polymer films. Adapted from M. H. Stenzel, Formation of regular honeycomb pattern porous film by self-organization, *Australian Journal of Chemistry*, 2003, **55**, 239–243.
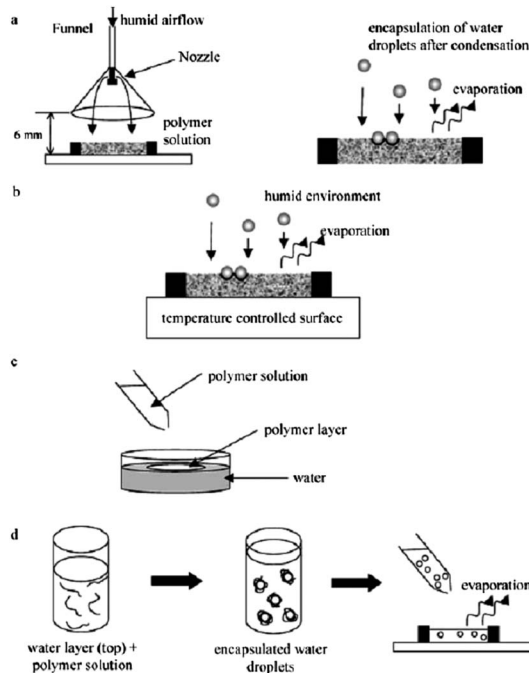
Fig. 3 Schematic representation of various casting techniques based on the breath figure method for the preparation of honeycomb structured porous polymer films. (a) Airflow technique, (b) cold-stage casting technique, (c) casting on water technique, (d) emulsion technique. Reprinted from K. H. Wong, M. Hernández-Guerrero, A. M. Granville, T. P. Davis, C. Barner-Kowollik and M. H. Stenzel, Water assisted formation of honeycomb structured porous films, *Journal of Porous Materials*, 2006, **13**, 213–223.

dynamic evaporating system. Humidity content, flow rate, distance and angle of direction of the air are control variables in this technique.[34]

Casting on water technique. Not only solid substrates have been used for honeycomb membrane casting. The air–water interface is a surface that can be used to produce self-standing membranes. In this technique, the floating membranes are recovered with a glass slide. Shimomura and co-workers successfully used the air/water interface to produce honeycomb membranes from an amphiphilic copolymer, namely, dodecylacrylamide and ω-carboxyhexylacrylamide in benzene.[35] The area and thickness of the membranes were controlled both by the volume of spread of the solution and water temperature. Film thickness ranged from 685 to 1260 nm. Connal *et al.* further modified the technique by pre-casting a thin layer of the polymer solution in water followed by further casting of the same solution.[36] Davis and co-workers obtained regular honeycomb membranes when casting a PS-comb polymer at the air–aqueous solution interface.[34]

Cold-stage casting technique. In this variation of the basic "breath figures" technique, the temperature of the solution and the substrate can be controlled in order to enhance condensation.[37–39] A cold-casting cell is used for that purpose. The solid casting substrate is placed on the cold-stage to control temperature below ambient conditions. A more substantial condensation and increase in viscosity occur due to a lower temperature.

Moreover, the interfacial behaviour between the solution and the condensed water droplets is also affected. The cold-stage can be a surface or the air–water interface for the casting on water technique. Highly regular membranes of poly(p-phenylenevinylene) and polythiophene of tenths of mm^2 were obtained when controlling the temperature of the substrate (40% saccharose in water) to temperatures from 5 °C to 3 °C.[37]

Emulsion technique. Finally, in the "emulsion technique" variation, water (or an aqueous solution) is directly introduced into a polymer solution.[40–42] The system is generally homogenized by sonication. In this way, honeycomb structured membranes from homopolymers such as cellulose acetate butyrate, monocarboxylated polystyrene and poly(methyl methacrylate) (PMMA) have been successfully obtained from THF solutions under a dry environment (RH < 30%).[43] PS and PMMA honeycomb membranes were also obtained when injecting sucrose aqueous solutions into benzene solutions of either polymer.[41] PS based comb polymers in non-polar solvents such as carbon disulfide in emulsion with up to 50% v/v of water have also rendered highly regular honeycomb membranes.[34]

Recently, a Pickering-emulsion effect was introduced into the "breath figures" method to obtain particle-functionalized membranes. Silica and polystyrene particles and also poly-(NIPAAm)-co-acrylic acid microgels were used as stabilizing agents in aiding the formation of ordered membranes.[44]

Combination with other methods: spin coating and dip-coating. Spin coating and dip-coating have been widely used in the laboratory to obtain uniform films.[45–47] The breath figure technique has been combined with spin coating in humid conditions.[48–51] Elongated pores rather than circular pores are obtained by combining both approaches. High spinning rates have been shown to be beneficial to obtain highly regular porous structures, while lower spinning rates allow for coalescence to happen. Using the combination of these two approaches, PET-fluorinated films were observed to be distinctively more ordered at high spinning rates from 2000 to 3000 rpm compared with films obtained at 1000 rpm.[52] Munoz-Bonilla and co-workers were able to prepare porous membranes from an amphiphilic ABC triblock copolymer poly(2,3,4,5,6-pentafluorostyrene)-b-polystyrene-b-poly[(ethylene glycol) methyl ether methacrylate] (PS5F(21)-b-PS31-b-PPEGMA(38)) mixed with a high molecular weight polystyrene by spin coating under humid conditions.[53]

As in the combined spin-coating-"breath figures" technique—the process of the combination of dip-coating with "breath figures" is performed under a highly humid environment. A graft copolymer styrene/(methacryloyl terminated PEG macromonomer) = 105/1 dissolved in CHCl$_3$ has been successfully used to obtain pores of about 1.5 μm and 900 nm depth with a pulling speed of 500 cm min^{-1} under a humid environment of 70% RH. For this system, no ordered films were obtained by the conventional casting method. Therefore, the combination of the two methods is beneficial to structure some materials.[54]

Variables and control of membrane properties

Variables such as humidity, solvent, polymer–solvent interactions, concentration, temperature, substrate, type of polymer,

polymer architecture and molecular weight have been identified as particularly crucial for the quality and properties of the membranes.[55] In fact, the spectrum of possible interplay of all the variables is broad. By controlling these variables, the quality, pore size, spacing between pores and thickness of the membranes can be tuned and optimized. Multilayered or mono-layered arrays of pores are also intimately related to the process variables.

In this section, we present some general observations and results from studies that have controlled the aforementioned variables in order to optimize the quality of honeycomb membranes. It must also be pointed out that each casting system (polymer solution and conditions) is unique and, therefore, in some cases no definite conclusions on the effect of each variable can be drawn.

Humidity. Evidently, one of the most important variables of the technique is the level of humidity. Environments with a relative humidity of 50% or higher are necessary to promote favourable condensation.[56,57] A certain degree of control of the pore size can be achieved by regulating humidity during membrane casting. A trend is observed in which the size of the pores in the films increases almost in a linear fashion with humidity.[58] In contrast, vast condensation at high humidity may result in the coalescence of water droplets yielding a polydisperse pore size distribution. This was the case for films from a series of amphiphilic block copolymers of polystyrene-b-poly(N,N-dimethylacrylamide) (PS-b-PDMA) with increasing hydrophilic blocks.[59] The strong interaction of the hydrophilic block of the amphiphiles resulted in a decrease in pore regularity. The pore size increased with humidity, from 250 to 750 nm to 1 μm for 60% RH and 65% RH, respectively. A further pore size increase was observed at 80% and 90% RH. However, the ordering of pores was affected at these humidity values (Fig. 4).

Solvent. In order to obtain highly regular porous films, non-polar and highly volatile solvents are preferred. The most common solvents used for the "breath figures" technique include carbon disulfide,[60] dichloromethane,[61] chloroform,[62,63] benzene,[64] toluene,[65,66] tetrahydrofuran[67,68] and freon[69] among others. Mixtures of these solvents have also been used to enable solubilization of some polymers to apply the "breath figures" technique.
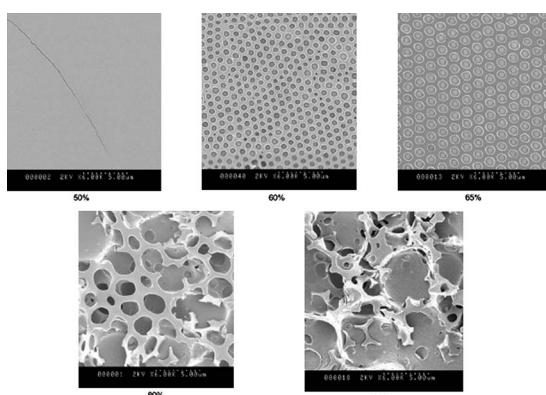
The evaporation rate of the solvent influences the whole casting process and the condensation. The conformation of the polymer in solution, the surface tension of the solution, viscosity, the facility of the polymer to undergo Brownian motion and the restriction to polymer movement by intermolecular forces are closely associated with the solvent and determine the quality of the membranes.[70] Billon et al. found a correlation between the wet thickness (i.e. the height of the solution) and the evaporation rate in the formation of multilayered films. A slow evaporation is believed to allow for the sinking of a first condensed layer of droplets, leaving space for the creation of a second layer on top of the solution. The authors demonstrated the formation of multilayered films even when using high density solvents. In agreement with other works, in this work it is believed that thermocapillary and Marangoni forces cause the droplets to submerge and create the hexagonal array.[71]

Concentration. With regard to the concentration of polymer solutions for the "breath figures" technique, it is worth noting that the majority of studies focus mainly on weight concentrations and not on molar concentrations. Therefore, detailed studies keeping a constant molar concentration for various polymers with different molecular weights are required. Here we present some examples where the concentration of the polymer in solution had a role in determining pore size, quality, and formation of mono- or multilayers for the honeycomb films.

Concentration and pore size. The polymer concentration in solution and the pore size follow the relationship $PS = k/C$, where PS is the pore size in the film, K is a constant dependent on the type of polymeric material used and C is the concentration of the polymer solution. Stenzel observed a strong relationship between the pore size and the concentration in solution when using amphiphiles, whereas less influence was observed when using various concentrations of star polymers.[55]

Concentration and film quality. In other cases, the concentration is an important variable for the quality of the film. Polycarbonate honeycomb membranes were successfully obtained by casting from chloroform in the concentration range of 0.03 g mL^{-1} to 0.09 g mL^{-1}. However, the order and regularity were lost at 0.1 g mL^{-1}. Poly(L-lactide)-b-poly(ethylene glycol) (PLEG) honeycomb membranes were obtained only at concentrations below 0.5 g L^{-1}.[72]

Concentration and formation of mono- or multilayers. The concentration of the polymer in solution also affects the formation of multi- or mono-layered porous membranes. A honeycomb membrane with a monolayer was obtained when using 0.5 mg mL^{-1} of a dendronized block copolymer polyethylene oxide-b-polydimethylacrylamide (PEO$_{113}$-b-PDMA$_{82}$) in chloroform. For the same polymer, a higher concentration of around 2 mg mL^{-1} rendered membranes with multi-layers.[73]

Fig. 4 SEM images of membranes from PS$_{75}$-b-PDMA$_{30}$ (10 g L^{-1} in 70 : 30 v/v% CS$_2$–CH$_2$Cl$_2$) at constant airflow and different relative humidity values. Re-printed from K. H. Wong, T. P. Davis, C. Barner-Kowollik and M. H. Stenzel, Honeycomb structured porous films from amphiphilic block copolymers prepared via RAFT polymerization, *Polymer*, 2007, **48**, 4950–4065.

Temperature. The temperature control during the casting process affects the evaporation of the solvent, condensation, surface tension, viscosity of the polymer solution, solubility, conformation of the polymer and precipitation at the water–solution interface. Therefore, various authors have focused on the control of the temperature of the casting substrate and polymer solution in order to optimize the production of honeycomb regular membranes.[74] Cold casting cells or cold aqueous solutions have been used to control this variable (see also the previous section for cold-stage casting). By using a cold-stage for casting, Angus *et al.* found favourable conditions to obtain honeycomb membranes from a 5-arm PS star chloroform solution.[38]

The temperature of the substrate (40% saccharose in water) was controlled from temperatures around 5 to 3 °C in order to obtain good quality honeycomb films from a mixture of 2% xylene solutions of poly(*p*-phenylene-vinylene) and poly-thiophene.[37] For a poly(lactide-*co*-glycolic)acid (90 : 10) in chloroform solution, honeycomb membranes with bigger and deeper pores were obtained at low temperatures compared with the higher temperatures.[39]

Vacuum. Another variable that has been controlled in order to obtain highly regular porous membranes is vacuum. Li and co-workers produced porous membranes with voids between 5.6 and 17.1 μm by controlling the pressure inside a casting chamber. The low pressure in the controlled humidity chamber favoured the evaporation of the solvent and the condensation of water droplets for the templating of pores.[75]

Substrate. Undoubtedly, the substrate or surface where the polymer solution in the "breath figures" technique is deposited plays a very important role in the regularity and final quality of the pore array in the membranes. The honeycomb films can be obtained on a wide range of hydrophilic and hydrophobic or hydrophobized surfaces such as glass, silicon wafers, quartz, mica, water, indium tin oxide, silanized glass, gold-coated TEM grids, glassy carbon electrodes and non-flat substrates are examples of the materials that have been used to produce honeycomb membranes.[58,76–78] Polymeric substrates such as PVC and polymethylmethacrylate surfaces have also been tested.[71] Various works have shown the effect of the substrate on membrane morphology. Valiayaveettil and co-workers used clean glass, epoxy, amine terminated and dendrimer functionalized glass as well as silicon wafers to cast a poly(*p*-phenylene) with pyridine chloroform solution. In this work, honeycomb membranes were obtained from glass and silicon wafers. In contrast, ring patterning, low pore density or net-type structures were obtained from the epoxy-treated, amine terminated and dendrimer functionalized glasses, respectively.[76] Connal *et al.* observed a strong dependency on the type of TEM grid and the morphology of membranes obtained from a 19 arm poly(dimethylsiloxane) (PDMS). The PDMS seemed to be a very versatile material for the casting of very regular honeycomb membranes on various substrates such as kaolin and silica particles.[79] The surface of water has also been used as a plane for membrane casting (see the previous casting on water section). The membranes obtained from the air–water interface are self-standing, which makes them particularly interesting for

applications when a non-supported film is required. In another study, the effect of glass, silicon slides and mica was tested. The authors found mica to be the best substrate for the casting of dendronized block copolymers. Contact angle studies indicated that wetting is an important factor to obtain honeycomb structured films. In contrast to mica, less order was obtained for glass and silicon slides, as shown in Fig. 5.[92]

Polymer. Polymer properties are of course determinants of the final quality of the films. The average molecular weight, degree of branching, end-groups, impurities such as unreacted monomer, solvents and low molecular weight fractions affect chain flexibility (glass transition temperature) and influence the pore size, precipitation and stabilization of the water droplets. Therefore, many studies are dedicated to the synthesis of well-defined polymers to estimate the best conditions for the "breath figures" technique.,[80] For this purpose, various living/controlled polymerization techniques have been used. These techniques include, among others, Atom Transfer Radical Polymerization (ATRP),[81] Nitroxide Mediated Radical Polymerization,[82,83] and Reversible Addition Fragmentation Chain Transfer Polymerization (RAFT).[84–86] Stenzel and co-workers reported the use of well defined polymers such as block copolymers, comb polymers, star shaped and amphiphilic macromolecules prepared by living/controlled radical polymerization.[87–90] Hyperbranched polymers and dendronized block-copolymers can also form regular porous membranes.[91,92] In general, these architectures that adopt a spherical shape in solution allowed the production of highly regular porous membranes. Compared with linear PS, a certain degree of branching density, a high molecular weight and low viscosity have been the key factors to obtain honeycomb membranes, as observed in 1999 by François and co-workers.[93,94] However, other studies show that under the right conditions regular honeycomb porous films from linear polystyrene without polar end-groups in the range 100–200 K can be obtained.[95,96] Other authors have highlighted the importance of end-groups in polystyrene for the formation of honeycomb films.[97]

Amphiphilic polymers and substructures in the films. A special note needs to be made for polymers with a certain degree of hydrophilicity as the regularity of the pores seems to be dependent on the hydrophobic to hydrophilic ratio due to the strong interaction of the water condensates with the hydrophilic part of the polymers. *N*,*N*-Dimethylacetamide, acrylic acid, acryloyl phosphorylcholine or *N*-isopropyl acrylamide have been used
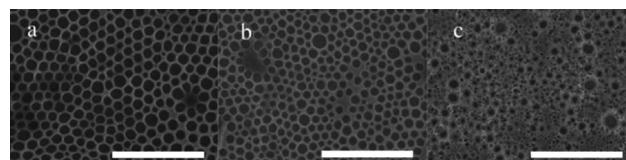
Fig. 5 SEM images of the honeycomb structure of films prepared at 18 °C and 90% RH by spreading 40 μL of the copolymer solution (0.75 mg mL^{-1}) onto (a) mica, (b) glass, and (c) silicon plates, respectively. The bar is 20 μm. Re-printed from C. Xia Cheng, Y. Tian, Y. Qiao Shi, R. Pei Tang and F. Xi, Porous polymer films and honeycomb structures based on amphiphilic dendronized block copolymers, *Langmuir*, 2005, **21**, 6576–6581.
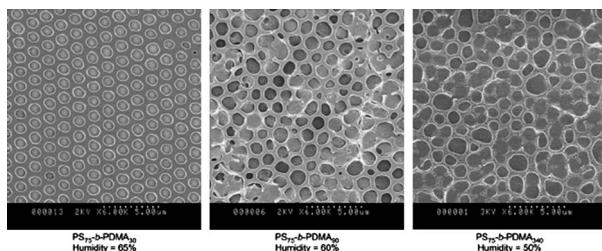
Fig. 6 SEM images of films cast from PS-*b*-PDMS (10 g L⁻¹ in CS₂/CH₂Cl₂ 70 : 30 v/v%) showing that the regularity is compromised with increasing length of the hydrophilic PDMA block. Re-printed from K. H. Wong, T. P. Davis, C. Barner-Kowollik and M. H. Stenzel, Honeycomb structured porous films from amphiphilic block copolymers prepared *via* RAFT polymerization, *Polymer*, 2007, **48**, 4950–4965.

Fig. 7 Substructure in porous films from amphiphilic block copolymers. (A) Growth of hydrophobic bacteria *Psychrobacter* sp. SW5H accumulated around the pores of honeycomb structured films and (B) growth of hydrophilic bacteria *Vibrio* sp. inside the pores of the membranes. Reprinted from M. H. Stenzel, C. Barner-Kowollik and T. P. Davis, Formation of honeycomb-structured, porous films *via* breath figures with different polymer architectures, *Journal of Polymer Science Part A-Polymer Chemistry*, 2006, **44**(8), 2363–2375.

together with polystyrene as the hydrophobic block for membrane casting.[98,99]

Light-emitting rod-coil block copolymers were used to drop cast honeycomb porous membranes with a two-dimensional structure. The obtained films were used as templates for two-dimensional arrays of aluminium microdots.[100] In another work using block copolymers, side-chain liquid crystalline block polymers with a styrene-*co*-maleic anhydride alternating block were employed.[101] Honeycomb membranes with a thickness of 1 μm and pores from 20 to 120 nm of amphiphilic block copolymers of polystyrene-*b*-polyacrylic acid were successfully cast from THF solution.[102] Thermoresponsive polystyrene-*b*-poly(*N*-isopropyl acrylamide) amphiphilic block copolymers were also used for membrane casting. The regularity of the produced membranes was compromised by the size of the hydrophilic block, which was arranged around the pores, while the surface of the membranes contained the hydrophobic part.[99] The amphiphilic di-block copolymers polystyrene-*b*-poly(*N*,*N*-dimethylacrylamide) (PS-*b*-PDMA) were more sensitive towards humidity with increasing hydrophilic block. The regularity of the films increased with smaller hydrophilic block.[59] A greater PEG content in amphiphilic graft copolymers polystyrene/polyethylene glycol (PS/PEG) (10, 30, 100 mol mol⁻¹) led to sponge-like structured membranes in contrast to the polymers with the lowest PEG content that produced regular membranes (Fig. 6).[54]

Well-defined polymethylene-*b*-polystyrene copolymers with different ratios were cast from CS₂ to render honeycomb films with pore sizes ranging from 1.2 to 2.5 μm. When cast at 28 °C, the films had smaller pores surrounding the hexagonally packed micropores.[103] An amphiphilic copolymer containing ruthenium tris(bipyridyl) helped in the formation of highly ordered honeycomb films. An effect on the pore size and the height of the porous structure was also observed. Both parameters, pore size and height, increased when increasing the content of the copolymer.[104] The substructure created in honeycomb films when using amphiphilic block copolymers was tested with a range of bacteria. *Psychrobacter* sp. SW5H has shown a preferential adhesion to hydrophobic surfaces.[105] In contrast, *Vibrio* sp. prefers hydrophilic surfaces. These two types of bacteria were grown onto honeycomb structured films. The authors observed accumulation of the hydrophobic surface loving bacteria around the pores, whereas the hydrophilic bacteria grew inside the pores of the membranes (see Fig. 7).[106]

Hierarchical structures were obtained from diblock copolymers poly(*n*-butyl acrylate)-*b*-polystyrene or poly(*tert*-butyl acrylate)-*b*-polystyrene that were synthesized *via* nitroxide mediated polymerization. A nanostructuration of the acrylate-based coil-coil diblock copolymer was observed inside the walls of the porous membranes.[107]

Concentration and polymer structure were two important variables necessary to obtain regular films from glycopolymers based on PS and 2-(2-,3-,4-,6-tetra-*O*-acetyl-beta-D-glucosyloxy) ethyl methacrylate) AcGEMA with linear PS-*b*-PAcGEMA/PS-*co*-PAcGEMA or PS-*b*-(PHEMA-*g*-PAcGEMA) having comb-like architectures. In this study, the authors obtained honeycomb films only from the glycopolymers with a long PAcGEMA content.[108]

Star polymers and number of arms. Highly branched polymers such as star polymers have a good ability to stabilize the droplet array during precipitation. An influence on the number of arms in these polymers has been observed. Pore sizes of 250 nm were obtained when casting an 18-arm PS star. By contrast, PS star polymers with the same molecular weight (around 10 000 g mol⁻¹) but with 5 arms rendered membranes with pores around 800 nm.[88]

Surface tension and use of surface tension modifiers. Early in the area, a very complete report on mesoscopic patterning extended the applicability of the breath-figures technique to a wide range of amphiphilic polymers such as DNA/amphiphile complexes, saccharide vinyl polymers, photoresponsive and electrically conducting complexes. The ability of the complexes to reduce surface tension between neighbouring water droplets was pointed out as the critical factor to obtain highly ordered films.[58] The importance of the presence of a surfactant molecule was highlighted. A phospholipid, dioleoylphosphatidylethanolamine (DOPE), and other phosphatidylcholines were used in this study. The results clearly indicate that the HLB value and interfacial tension greatly affect the stability of water droplets. DOPE, which has a low HLB value and can maintain high interfacial tension (>10 mN m⁻¹) during solvent evaporation, was shown to aid in the formation of poly(D,L-lactic acid). Similar to DOPE, dierucoylphosphatidylcholine (DEPC) and dierucoylphosphatidylethanolamine (DEPE), which have a high

interfacial tension, were also beneficial in preparing honeycomb films.[109] In another report from the same research group, a series of amphiphilic polymers based on PS and polyacrylamide with different ratios were synthesized and studied regarding their ability to form ordered films. The authors observed a beneficial decrease in the surface tension of the solution with increasing hydrophilic ratio. From this study, it is clear that the quality of the membranes can be controlled by the surface tension of the polymer solution and water.[110] An amphiphilic polymer containing ruthenium tris(bipyridyl) added to polystyrene solutions was necessary to obtain films with order. The pore diameter and height increased with higher amount of the amphiphilic polymer in solution, reaching a limit amount in which the order was lost and the pore size decreased.[111]

Characterization techniques

Once produced by the "breath figures" technique, the membranes can be characterized mainly by microscopy techniques or mathematical approaches. The microscopy techniques were the first option to study the membrane surface; however, without any further analysis, the microscopy approach can be considered subjective in determining the real quality of the membranes in terms of pore spatial arrangement and pore size. Due to this fact, some mathematical approaches are now used in order to quantify the quality of the films. Here we present both approaches that, far from being inclusive, are rather complementary to each other.

Analysis of the surface by microscopy techniques

Honeycomb membranes can be characterized by microscopy techniques, light scattering,[112] and various mathematical approaches. The surface topography can be studied by optical microscopy,[112–114] scanning electron microscopy (SEM)[113] 3D SEM,[115] atomic force microscopy (AFM),[48,113] lateral force microscopy (LFM),[49] fluorescence microscopy, confocal microscopy, transmission electron microscopy (TEM),[116,117] and X-ray photoemission electron microscopy (XPEEM).[48] Among all these techniques, optical microscopy has been the first option for the inspection of the porous membranes due to its availability, low cost and ease of use. When higher magnifications are needed, SEM has been the technique of choice. Moreover, by removing the top layer of the membranes with adhesive tape, this technique allows the study of the lower layers. Likewise, analysis of the cross section of the membranes can be done with SEM. However, it normally implies sample preparation (conductive coating) to observe membranes from non-conductive polymers. AFM as a non-destructive and high resolution method has been applied to obtain 3D profiles of the surface of the membranes. An advantage of this technique is the possibility to study membranes in a hydrated state or immersed in a liquid, which is useful for membranes from stimuli responsive polymers. The tapping mode is suggested for the membranes, as they are made from soft polymers. For the AFM analysis, the tip choice is crucial as some scanning artifacts could appear if the radius of the tip is bigger or around the same size as the pores. Possibly, a disadvantage of AFM is that the scanning sizes are smaller compared with the images that can be obtained from SEM.

When membranes are labelled with fluorescent compounds, fluorescence microscopy has been useful in their analysis.[118] Confocal microscopy is of particular help when studying membranes with multilayers. The order in each layer and defects in the layers can be detected with this technique by studying the XY or XZ planes and reconstructing 3D images.

Analysis of honeycomb structured porous films by mathematical approaches

An approach called Quantitative Virtual Light Scattering (QVLS) has been used by Davis and co-workers to quantify the quality of honeycomb structured porous membranes.[38] This simple method is based on the principle of light scattering; however, this is not an experimental but rather a virtual and non-destructive tool that is applied to microscopy images of the membranes. This mathematical approach is a good method for the researcher to use, as it can give some feedback and direction for studies and provide variable control to obtain better quality membranes. This technique uses Fourier transformation to assess the order (spatial arrangement) and size polydispersity of the pores in the membranes. The calculations are based on a hexagonal lattice in which there is a 60° angle of alignment between three pores. This method also takes into account that in the hexagonal array, a pore is surrounded by six other pores (*i.e.* it studies 1st order neighbours and a central pore; see Fig. 8).

Two coefficients, namely SPAN $\sigma(R)$ and THETA $\sigma(\Theta)$, give the degree of repeated pore to pore distances and the degree of repeated angles, respectively. SPAN and THETA coefficients range from an approximate value between 0.0–0.4 and 0.0–9.0, respectively. The lower the values for both coefficients, the better the quality of the membranes. In addition, the quality of the membrane is also displayed in a graphic that shows light scattering patterns. A 'halo' geometry shows repeated distances but not repeated angles. A good quality membrane with both repeated distances and repeated angles would display six peaks, representing three categories of repeated angles/distances (3 peaks) with the corresponding mirror image (3 more peaks).

Likewise, frequency distribution plots 2D and 3D (Fig. 9) contour plots of the first order near-neighbouring $X–Y$ centers are obtained.
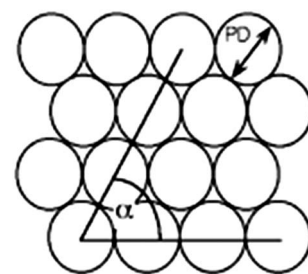
Fig. 8 The ideal hexagonal arrangement in the pores of a honeycomb structured porous film where alpha is the angle among three adjacent pores and PD is the pore diameter. Reprinted from S. D. Angus and T. P. Davis, Polymer surface design and infomatics: facile microscopy/image analysis techniques for self-organizing microporous polymer film characterization, *Langmuir*, 2002, **18**, 9547–9553.
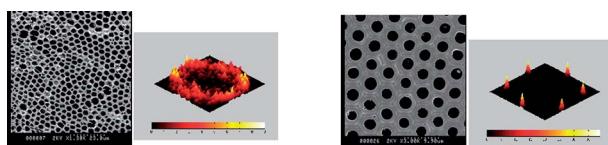
Fig. 9 Honeycomb structured porous films and 3D contour plots from the QVLS analysis showing a halo geometry (left) indicating some repeated distances but not repeated angles and 6 peaks (right) resulting from the ideal hexagonal array in the film. Reprinted from S. D. Angus and T. P. Davis, Polymer surface design and infomatics: facile microscopy/image analysis techniques for self-organizing microporous polymer film characterization, *Langmuir*, 2002, **18**, 9547–9553.
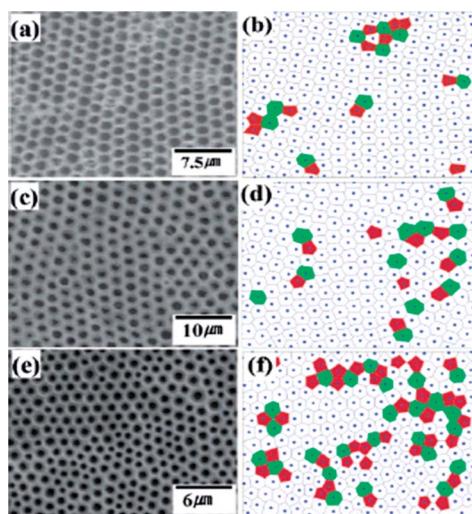
Fig. 10 Schematic representation of the application of the Voronoi polygon method to assess the order of honeycomb structured porous films. (a, c, e) SEM images of the porous membranes, (b, d, f) corresponding Voronoi diagrams. Different conditions and solvents were used for each membrane (a) casting from chloroform, (c) casting from THF, and (e) spin coating from THF. Re-printed from M. S. Park and J. K. Kim, Breath figure patterns prepared by spin coating in a dry environment, *Langmuir*, 2004, **205**, 5347–5352.

The Voronoi polygon method is another option to assess the regularity and the presence of defects in the membranes. This method is also based on the use of microscope images.[43] It calculates the probability of the occurrence of five (P_5), six (perfect hexagonal lattice) (P_6) or seven (P_7) neighbors around one pore (see Fig. 10). The conformational entropy of the pores in the membranes is calculated and is compared with the conformational entropy for an ideal hexagonal lattice ($S = 0$) and a randomly organized array of pores ($S = 1.71$). This Voronoi polygon method has been applied in a comparison of the order in films produced from different solvents or methods. Conformational entropy values close to zero indicate that a membrane has a hexagonal array.

Stability of the membranes

Due to the fact that the process of formation of honeycomb porous membranes is merely physical, the membranes are prone to damage by external factors such as solvent or high temperatures. In order to address this situation, blends of materials, materials such as highly stable polymers and cross-linking have been used to impart stability. It is worth mentioning that all these strategies have opened a window of opportunity for applications of the membranes.

Blending

More resistant membranes were obtained from the blending of PS star polymers and PMMA-star microgels with their linear counterparts.[88,36] Polysulfone, being a highly stable polymer, was used to produce porous membranes.[119] This material is resistant to high temperatures and can withstand acids, alkali, saline solutions and surfactants.

Cross-linking

Highly stable membranes were formed from an amphiphilic copolymer and an oligomer, Bisphenol A, with photo-cross-linkable epoxy groups. After UV cross-linking, the membranes were resistant to various organic solvents and only a decrease to half the size of the pores was observed.[120] Photo-cross-linking was an approach followed to stabilize membranes from a four-arm star methacrylate modified poly(D,L-Lactide).[121] Li *et al.* UV irradiated PS honeycomb membranes to improve their thermal and chemical stability. Upon irradiation, the membranes were resistant to various organic solvents and temperatures up to 250 °C. The exposure to UV also changed the hydrophobic character of the PS membranes to a more hydrophilic character.[122] The same approach was followed to crosslink membranes from a block copolymer from PS and polyacrylic acid.[123]

Honeycomb films have also been treated with 1,8-diaminooctane by immersion for a period of time. Twenty-four hours was shown to be sufficient for PS-maleic anhydride films to be stable to a range of solvents such as methanol (MeOH), chloroform ($CHCl_3$), carbon disulfide (CS_2), acetone, toluene, and tetrahydrofuran (THF).[128] Post-treatment of membranes to convert polyamic acid to polyimide (a highly stable material) was sufficient to impart thermal and chemical stability. The membranes were annealed at 300 °C without any damage. Pyrolysis and full decomposition of the polyimide membranes occurred at 400 °C and 449 °C–511 °C, respectively. The membranes were also stable upon immersion in various organic solvents and sulfuric acid for 2 weeks.[30]

Functionality in the membranes

A special section on membranes with functionality or enriched pores is presented below. The works in the area show the importance of functionalization techniques in imparting specific properties that make possible various applications for the membranes.

Honeycomb membranes can be functionalized to infuse them with characteristic properties for special applications. Various works have already achieved the modification of membranes by casting functionalized polymers and amphiphilic polymers, surface grafting,[158] and enrichment of the pores with other materials. The section on amphiphilic polymers and substructures in the films gives some examples of the polymers that

impart a substructure on the films. We further elaborate in this section.

Pore enrichment from functionalized polymers, amphiphilic polymers, ionomomers

Amino-terminated linear PS was used to obtain honeycomb membranes with pores enriched with amino groups. The same approach was used to obtain membranes from a luminescent chain-ended PS.[124]

Thermoresponsive amphiphilic block copolymers polystyrene-*block*-poly(*N*-isopropyl acrylamide) were used to obtain highly regular porous membranes with a varying composition at the surface and inside the pores. The authors found by contact angle measurements that the surface of the membranes reacted like a typical hydrophobic surface, whereas the pores were enriched in hydrophilic sequences.[99]

Highly ordered microporous membranes were functionalized by a one-step process by doping a surfactant-encapsulated polyoxometalate complex into a PS solution. The polyoxometalate complex accumulated inside the pores of the membranes. The authors have suggested this method as a facile alternative to functionalize the pores of membranes with other materials.[125] A methacryloyl galactose based polymer was used to obtain bioactive honeycomb membranes, where lectin assays were performed with peanut agglutinin that conjugated with the sugar moieties of the porous material, mostly inside the pores. The authors suggested this as a simple procedure for the patterning of proteins onto surfaces.[126]

Membranes from PS and a statistical glycopolymer with voids from 200 to 700 nm showed organization of the glycopolymer inside the pores, as confirmed by swelling of the material upon soft annealing in water, reaction with rhodamine isocyanate and lectin binding test with concanavalin A.[127]

Self-assembly of ionomer macromolecules based on PS into starlike micelles due to the non-solubility of the ionic end-chains in the organic solvent allowed for functionalization of the pores, as shown in Fig. 11.[71]
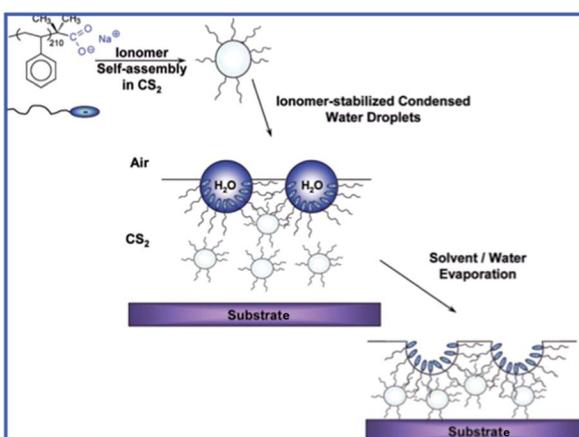

Fig. 11 Representation of the formation of the honeycomb structured films by ionomer-stabilized condensed water droplets. The pores possess a functionality. Re-printed from L. Billon, M. Manguian, V. Pellerin, M. Joubert, O. Eterradossi and H. Garay, Tailoring highly ordered honeycomb films based on ionomer macromolecules by the bottom-up approach, *Macromolecules*, 2009, **42**, 345–356.

Well-defined poly(*n*-butyl acrylate)-*block*-polystyrene or poly(*tert*-butyl acrylate)-*block*-polystyrene copolymers were used to fabricate hierarchically ordered microporous films by the breath figures technique. Ordering of the pores was observed over an area of 1 cm². The films had two levels of structuring: the hexagonal morphology obtained when casting the polymers and the acrylate coil-coil diblock copolymer self-assembled around the walls of the microporous array. The nanostructuration was achieved by using very well-defined diblock polymers with different block ratios to attain lamellar or cylindrical morphology. Both levels of structuring were influenced by features of the polymeric material such as interaction parameter, glass transition temperature and monomer weight fraction.[107]

By surface grafting

Reversible Addition Fragmentation Chain Transfer Polymerization was used to graft glycopolymer chains (NIPAAm and *N*-acryloyl glucosamine) onto cross-linked honeycomb membranes from poly(styrene-*co*-maleic anhydride). The membranes showed selective recognition and binding to concanavalin A above the LCST.[128] Carbohydrate-monomers were successfully grafted to honeycomb structured membranes prepared from an amphiphilic block copolymer of poly(styrene-*b*-(2-hydroxyethyl methacrylate)). The hydroxyl groups inside the pores were used as anchoring points for the grafting done by atom transfer radical polymerization. This is an interesting approach that allows the production of microarrays.[129] Hydrophobic porous honeycomb membranes from PS stars synthesized with ATRP were functionalized *via* surface grafting with polyglycidyl methacrylate chains, taking advantage of the living polymer chain end groups. The functionalized membranes were then used as the base for various surfaces having bis-alcohol groups or a model biomolecule, namely, (biotinamido)pentylamine.[130] Stenzel and co-workers produced reactive honeycomb structured membranes from amphiphilic block copolymers that allowed for a high functionality inside the pores for the attachment of proteins such as streptavidin (see Fig. 12).[131]

BODIPY-functionalized or amino functionalized PS, the latter synthesized with a TEMPO modified initiator, were successfully used to obtain honeycomb films. The presence of BODIPY was evidenced by thermal treatment to obtain flat films with spots of fluorescent dye in the position corresponding to the cavities on the films. After reaction with fluorescamine, the presence of the amino functionality mainly inside the pores was evidenced. These approaches to impart certain functionality to the films are currently being extended to some biological molecules.[124]

Hierarchical structures and bicomponent arrays

Microporous membranes were decorated with nanostructured block copolymers by combining the "breath figures" method with copolymer self-assembly through microphase separation at the nanometer scale. One advantage of this technique is the ability to vary the surface chemical composition through surface rearrangement by annealing under dry or humid air.[132]

Bicomponent arrays with honeycomb structure of two photoluminescent polymers were achieved by casting a polyfluorene copolymer. After casting the polyfluorene membranes by the
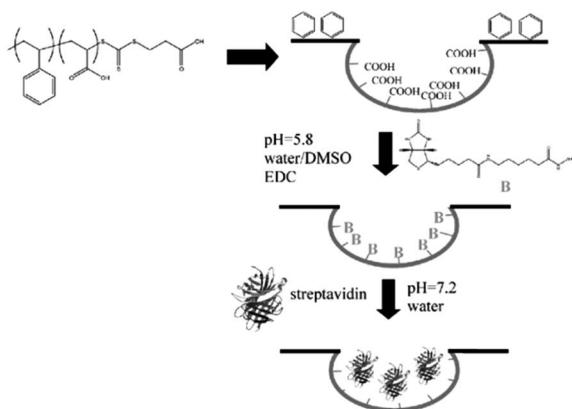
Fig. 12 Synthetic approach to a streptavidin microarray with immobilization of protein selectively in the pores. Re-printed from E. H. Min, K. H. Wong and M. H. Stenzel, Microwells with patterned proteins by a self-assembly process during honeycomb structured porous films, *Adv. Mater.*, 2008, **20**(18), 3350–3556.

breath figure technique, they were made resistant to organic solvents by annealing using a layer of polydimethylsiloxane with a curing agent to protect the morphology of the films. In this way, another polymer, in this case a polyphenylenevinylene, was dropped on top of the film to obtain hexagonal arrayed films in which the external area was mainly the polyfluorene based polymer and the internal area the polyphenylenevinylene.[133]

Membranes with switchable behavior

PS and poly(2-vinylpyridine) (P2VP) in THF solution have been used to produce honeycomb structured membranes with switchable topography. P2VP has a hygroscopic behavior; therefore, when exposed to water, the interior of the membrane rich in this polymer became swollen creating 'island-like' protrusions. Upon drying at 60 °C, the protrusions disappeared. The honeycomb membranes were also exposed to the vapors of organic solvents. For the case of good solvents for PS such as carbon disulfide, toluene and THF, protrusions were observed. However, when chloroform, methyl ethyl ketone and dimethylformamide were used, the 'island-like' protrusions ordered back to hexagonally arranged pores (see Fig. 13).[134]

Mimicking wood

In order to mimic a wood cell wall, lignin was adsorbed onto cellulose I (from a culture of G. xylinus) and cellulose II (from deacetylation of cellulose triacetate) honeycomb films. The honeycomb films were immersed into an acetic acid lignin solution overnight, washed to remove non-adsorbed lignin and subjected to bromine, which reacts with lignin. Upon the analysis of the films, the authors observed lignin adsorption mainly on the surface of the films. Compared with non-patterned films, a better tensile strength was also obtained on the honeycomb films with lignin.[135]

Blue-light emitting membranes

Blue light emitting porous membranes with superimposed structure were obtained from a 6 arm star poly(vinyldiphenylquinoline)
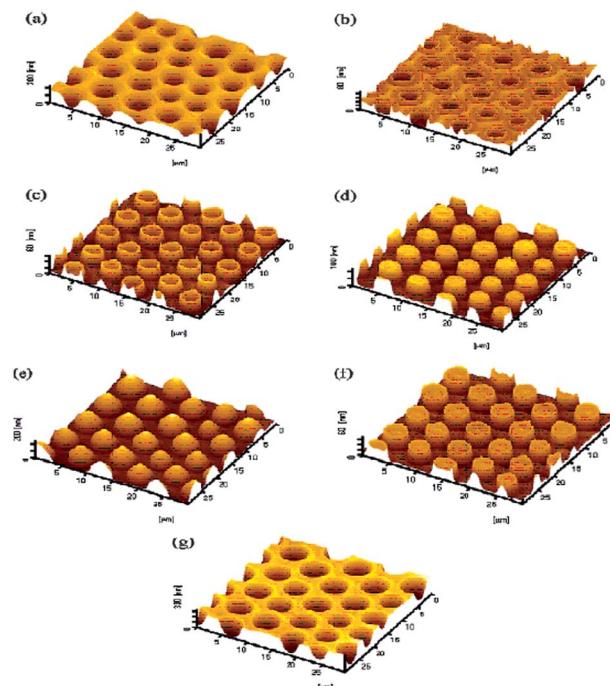
Fig. 13 AFM images showing the 3D topography of porous films with reversible switchable behaviour when exposed to solvent vapors (a) cast honeycomb film, (b–e) after exposure to CS₂ vapor for 10 min, 15 min, 20 min; and (f–g) after exposure to chloroform for 5 min and 10 min, respectively. Re-printed from L. Cui, Y. Xuan, X. Li, Y. Ding, B. Li and Y. Han, Polymer surfaces with reversibly switchable ordered morphology, *Langmuir*, 2005, **21**, 11696–11703.

and amphiphilic poly(*p*-phenylene) polymers. The membranes display a hexagonal array of pores of around 1 μm.[136] Upon excitation at a wavelength of 488 nm, the emission spectra showed maxima of 565 nm and 645 nm. The emission at 640 and at 740 nm was irregular throughout the membranes; however, when both fluorescence photographs are combined, distinct locations of emission between 640 nm and 740 nm are displayed. These confocal fluorescence microscopy results show that the membranes have two distinct regions of emission, an indication of the superimposed structure.

Applications and promising applications

Honeycomb membranes, due to their morphology, have been applied in various fields. Furthermore, the membranes may have many potential applications including filtration,[137] super-hydrophobic and self-cleaning surfaces, cell culturing and scaffolds for tissue engineering,[138] bioassays, templates for soft-lithography,[97] photonics, optoelectronics,[74] iridescent or bio-mimetic materials,[139,140] and coatings.[140] In this section, we describe some of the studies that have focused in applying and suggesting applications for honeycomb structured membranes.

Photoelectric conversion and light emitting diodes

These membranes have already been used for photoelectric conversion. The porous hexagonal array in membranes from a light-emitting poly(distyryldimethylbenzene-*co*-triethylene

glycol) rod-coil copolymer resulted in an increase in a generated photocurrent compared with non-patterned membranes from the same material.[141] OLEDs were produced with honeycomb membranes used as soft-lithography templates. They had a hexagonal ordered array of electroluminescent spots of around 1 μm–1.5 μm with red, green and blue emission.[142]

Electronics and flexible films

A liquid crystalline fluorine substituted polyacetylene was successfully cast into honeycomb membranes from a chloroform solution under humid conditions compared with stripes and lattice patterns obtained under dry conditions. These films could have potential applications in the field of electronics and photonics.[143]

Flexible honeycomb films from silicone based branched copolymers PEGDMA-ran-PMMA-ran-PMPS and PEGDMA-ran-PMMA-ran-PTRIS were successfully obtained from the breath figure technique and by further cross-linking *via* the sol–gel process, which allowed for higher flexibility and higher solvent resistance. These materials have potential applications as digital displays.[144]

Templates for other structuring techniques

The "breath figures" technique has complemented other templating techniques such as lithography, providing it with masks for the structuring of complex materials. The top layer of membranes from polystyrene and an amphiphilic polymer was removed by using adhesive tape to obtain a pin-cushion pattern. A Pt/Pd catalyst was deposited onto the pin-cushion mask, which was then immersed in a silver nitrate aqueous solution. To obtain the final material, the polymer was removed by dissolution in chloroform revealing metallic ordered pin-cushion structures.[145] In later studies, nickel/phosphorous coated membranes[146] and zinc oxide pin-cushion structures were obtained. A study that followed used the same approach; however, the honeycomb membranes were coated with gold that acted as a catalyst followed by the dipping of the membranes in an aqueous solution of zinc nitrate.[147] Furthermore, benzene solutions of a 1 : 4 mixture of a copolymer dodecylacrylamide and ω-carboxyhex-ylacrylamide and poly(L-lactic acid) were used as a precursor to create lithographic patterns in PDMS that, after Pt deposition, gave rise to wrinkled surfaces.[148] Microprinting based on "breath figures" opens a window of opportunity for applications in microelectronics and molecular biology. In this combined approach, a honeycomb membrane is fabricated and reproduced as a positive mold with polydimethylsiloxane. The mold can then be used for printing of biomolecules.[149] Micropatterns on various substrates can be produced by using a novel breath figure lithographic technique. As an example, a gold mask with hexagonal array can be prepared from a honeycomb membrane so as to transfer the pattern onto a silicon wafer by inductively coupled plasma reactive ion etching.[150]

Honeycomb structured films of PS and a polyacrylamide derivative were used as dry-etching masks to create novel biomimetic surfaces. The membranes were attached to silicon substrates and the composite material (polymer-silicon) was then etched to yield bifunctional surfaces with nanospike arrays,

anti-reflective and superhydrophobic properties. This is a simple method to obtain structured surfaces that could be used as solar cells.[151]

Substrates for Raman spectroscopy

The "breath figure" method has also been used to prepare honeycomb structured materials with gold nanoparticles by drop-casting a gold nanoparticle dispersion onto a surfactant monolayer at the air–water interface. A potential application for these membranes could be enhanced Raman spectroscopy.[152] Strongly enhanced Raman scattering of rhodamine 6G was observed on silver triangular spikes that were prepared by honeycomb membranes of PS and an amphiphilic poly-acrylamide combined with vapor deposition.[153]

Cell culturing, scaffolding and other biomedical applications

Honeycomb membranes of poly(ε-caprolactone) showed good adhesion properties and selective adsorption inside the pores for fibronectin.[154] In contrast to flat membranes, cell attachment was observed for fibroblast L929 cells after 24 h of incubation onto honeycomb membranes of polystyrene-*b*-polyacrylic acid templated with polypyrrole (see Fig. 14). Better cell adhesion was observed in the membranes with smaller pore sizes.[155]

Compared with non-patterned flat films, honeycomb membranes have displayed good properties for cell culturing. Some examples include the use of poly(ε-caprolactone)–dode-cylacrylamide-ω-carboxyhexylacrylamide membranes with interconnected pores for cell culturing. The membranes with smallest pore size from a range of membranes with pores of around 5–16 μm showed a high focal cell adhesion and high secreted extracellular matrix.[156] The same material was further used to obtain bone-like hydroxyapatite.[157]

PS-PHEMA based honeycomb membranes with PNIPPAm inside the pores were used for studies on fibroblasts cell attachment where a better interaction between cells and the surface was observed for higher hydrophilicity.[158] Highly regular honeycomb films with pore sizes 6, 12, and 16 μm were used to culture mature and small hepatocytes. Both the surface topography and the pore size were critical values during the culturing. The film with pores around 16 μm showed the highest cell yield for small hepatocytes, while showing higher albumin production in mature hepatocytes. A similar value of albumin production in flat films and the
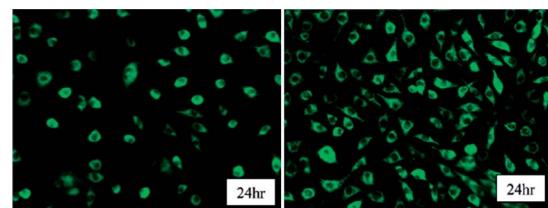
Fig. 14 Fibroblast attachment on honeycomb films after 24 h incubation. Pore size between 1 and 2 μm (left) and pore size below 1 μm (right). Reprinted from D. Beattie, K. H. Wong, C. Williams, L. A. Poole-Warren, T. P. Davis, C. Barner-Kowollik and M. H. Stenzel, Honeycomb-structured porous films from polypyrrole-containing block copolymers prepared *via* RAFT polymerization as a scaffold for cell growth, *Biomacromolecules*, 2006, **7**(4), 1072–1082.

honeycomb film was observed for small hepatocytes.[159] A commercially available block copolymer polystyrene-b-poly-butadiene-b-polystyrene was used to obtain honeycomb membranes that were photochemically cross-linked by UV-light. The membranes did not show cytotoxicity and upon exposure to radiation, the surface hydrophobicity decreased, which allowed for cell attachment and proliferation of the lung cancer cell line A549.[160]

Poly(lactide) honeycomb films were tested as a physical barrier for prevention of adhesion that generally occurs after intra-abdominal surgery during peritoneal healing. The results obtained by the author show that a poly(lactide) honeycomb film of around 10 μm thickness prevents adhesion in rat models and is suitable for endoscopic surgery.[161]

In the biomedical field, honeycomb membranes have been successfully used in animal models as postoperative physical barriers to prevent tissue adhesion. For example, honeycomb thin biodegradable films from poly(L-lactide-co-ε-caprolactone) were used as an adhesion barrier to prolong bleb survival after glaucoma filtration surgery. The honeycomb film attached to tissue from the structured porous side, while preventing adhesion of tissue from its smooth side. The honeycomb films promoted intraocular pressure reduction and bleb survival in glaucoma filtration surgery in rabbits with no complications. In contrast to some typical anti-scarring chemicals, when using the honeycomb films there were no abnormalities in the conjunctival epithelium.[162]

Surfaces with high hydrophobicity (Lotus leaf effect)

Honeycomb membranes display a highly hydrophobic character, which is the result of a hydrophobic polymer matrix combined with air entrapped inside the pores, the surface roughness, pore size and pore spacing. Due to the presence of a polymer and air, these porous membranes can be considered as composite materials in which both phases contribute to the contact angle.[99] This characteristic in honeycomb membranes is of importance. Surfaces with enhanced hydrophobicity are of great interest as they display dirt-repellent properties and therefore, the membranes may find applications as self-cleaning coatings. In this case, the high contact angle and surface roughness determine the self-cleaning power.[163] In the same efforts to achieve super-hydrophobic materials, fluorinated polymers were used to cast honeycomb membranes. The resulting membranes showed increasing hydrophobicity with decreasing pore sizes from 145° for pore sizes around 2 μm to 160° for pores of 300 nm. With optimization of the optical properties of the membranes, transparent films that could be used as optical coatings for windows were obtained.[164,165]

Patterning of microbeads, bioassays and diagnostic kits

An approach combining PS-beads and honeycomb membranes resulted in dissipative hierarchical structures, so called honeybeads.[166] Furthermore, honeycomb membranes with microbeads (PS, protein immobilized PS or anti-BSA-attached beads) have potential as bioassays or test kits.[167] For the same type of applications, membranes with Ag nanoparticles could be used.[168]

A recent approach towards biofunctional surfaces was addressed by Xu and co-workers. The authors prepared honeycomb membranes from PS/poly(ethylene glycol) PEG and studied the adsorption of bovine serum albumin. The results from laser scanning confocal microscopy showed that the pores were selectively enriched in protein-resistant PEG.[169]

Applications in sensors and catalysis

DNA-based honeycomb membranes that could be used as biosensors were produced by the "breath figures" technique by the encapsulation of DNA with a cationic surfactant bis-tetra-decyl dimethyl ammonium. The ability of the materials to form honeycomb membranes was high when controlling variables such as substrate, concentration and solvent. Circular dichroism tests showed that the DNA adopted a double helical B-form in the membranes.[170]

Photoresponsive honeycomb membranes of functionalized poly(acrylic acid)-spiropyran were used to create organic/inorganic porous membranes. The zwitterionic character of the polymer was used to absorb 100 ppm of $PdCl_2$. The organic matrix was then calcinated to produce palladium micro-rings. Applications for these membranes may include catalysis or specialized sensors.[171]

In blue-emitting and multicolor microporous membranes fluorene para-substituted styrene star-shaped polymers, a relatively uniform blue-emitting characteristic was observed on the P(St-Fl)8 microporous membrane. Such highly ordered structure led to a red shift in photophysical properties such as absorption and photoluminescence. Furthermore, multicolor microporous membranes were obtained via blending only 1% of green or red emitter into the P(St-Fl)8 membranes through efficient energy transfer.

Conclusions

The "breath figures" technique has made a big impact in the area of materials. Since its discovery, it has been widely accepted as a simple technique to structure porous membranes. It has also complemented other common lithographic techniques in the production of well-defined materials. The complexity of the variables' interplay during the process of formation has been the biggest drawback towards the industrial use of the technique. Important efforts in elucidating the mechanism of formation of the membranes have been made by the scientific community; however, no definite conclusions have been arrived at. Nevertheless, the process variables are well identified and include the solvent, concentration, polymer and its architecture, molecular weight, humidity, and substrate, among others. Some works have been devoted to quantifying the quality of the membranes to try to eliminate the subjectivity of the first approaches of analysis that involved comparisons between microscopy images from different films and a judgement by the naked eye. The membranes have been stabilized via physical and chemical methods, increasing in this way the possibilities for various applications in harsh environments. The functionalization of the membranes and substructures created by the polymers represents a synergistic approach to confer particular properties of interest for a wider number of applications. Catalysis, optics, filtration,

cell culture, scaffolding, coatings, nano- and micro-reactors, and diagnostic kits are listed among the wide number of potential applications for the porous materials obtained with the breath figures technique. Still young in the field, this technique promises to grow and be of more importance in biotechnology, bioengineering and chemistry. Nonetheless, it is nowadays one of the methods at the forefront of production of well characterized porous materials.

Notes and references

1 Rayleigh, *Nature*, 1911, **2169**(86), 416–417.
2 M. Sokuler, G. K. Auernhammer, M. Roth, C. J. Liu, E. Bonaccurso and H. F. Butt, *Langmuir*, 2010, **26**, 1544–1547.
3 H. Gau and S. Herminghaus, *Phys. Rev. Lett.*, 2000, **84**, 4156–4159.
4 M. Marcos-Martin, D. Beysens, J. P. Bouchaud, C. Godrèche and I. Yekutieli, *Phys. A*, 1995, **214**, 396–412.
5 D. Beysens and C. M. Knobler, *Phys. Rev. Lett.*, 1986, **57**, 1433–1436.
6 G. Widawski, M. Rawieso and B. François, *Nature*, 1994, **369**, 387–389.
7 C. T. Kresge, M. E. Leonowicz, W. J. Roth, J. C. Vartuli and J. S. Beck, *Nature*, 1992, **359**, 710–712.
8 W. Zhu, Y. Han and L. An, *Microporous Mesoporous Mater.*, 2004, 137–141.
9 E. Krämer, S. Förster, M. Göltner and M. Antonietti, *Langmuir*, 1998, **1**, 2027–2031.
10 T. Ohzono, T. Nishikawa and M. Shimomura, *J. Mater. Sci.*, 2004, **39**, 2243–2247.
11 T. Cao, F. Wei, X. Jiao, J. Chen, W. Liao, X. Zhao and W. Cao, *Langmuir*, 2003, **19**, 8127–8129.
12 G. M. Whitesides and Y. Xia, *Angew. Chem., Int. Ed.*, 1998, **37**, 550–575.
13 M. Campbell, D. N. Sharp, M. T. Harrison, R. G. Denning and A. J. Turberfield, *Nature*, 2000, **404**, 53–56.
14 A. Imhof and D. J. Pine, *Adv. Mater.*, 1998, **10**, 697–700.
15 S. Matsushita, T. Miwa and A. Fujishima, *Chem. Lett.*, 1997, 925–926.
16 S. H. Park and Y. Xia, *Adv. Mater.*, 1998, **10**, 1045–1046.
17 B. T. Holland, A. Stein and C. F. Blanford, *Science*, 1998, **281**, 538–540.
18 S. A. Davis, S. L. Burkett, N. H. Mendelson and S. Mann, *Nature*, 1997, **385**, 420–423.
19 Y. Uraki, J. Nemoto, H. Otsuk, Y. Tamai, J. Sugiyama, T. Kishimoto, M. Ubukata, H. Yabu, M. Tanaka and M. Shimomura, *Carbohydr. Polym.*, 2007, **69**, 1–6.
20 Z. Li, W. Zhao, Y. Liu, M. H. Rafailovich, J. Sokolov, K. Khougaz, A. Eisenberg and R. B. Lennox, *J. Am. Chem. Soc.*, 1996, **118**, 10892–10893.
21 M. Park, C. Harrison, P. M. Chaikin, R. A. Register and D. H. Adamson, *Science*, 1997, **276**, 1401–1404.
22 O. D. Velev, T. A. Jede, R. F. Lobo and A. M. Lenhoff, *Nature*, 1997, **389**, 447–448.
23 O. D. Velev and A. M. Lenhoff, *Curr. Opin. Colloid Interface Sci.*, 2000, **5**, 56–63.
24 O. D. Velev and E. W. Kaler, *Adv. Mater.*, 2000, **12**, 531–534.
25 M. Lee, B.-K. Cho, K. J. Ihn, W.-K. Lee, N.-K. Oh and W. C. Zin, *J. Am. Chem. Soc.*, 2001, **123**, 4647–4648.
26 S. A. Jenekhe and X. L. Chen, *Science*, 1999, **283**, 372–375.
27 H. Nishihara, S. R. Mukai, D. Yamashita and H. Tamon, *Chem. Mater.*, 2005, **17**, 683–689.
28 U. H. F. Bunz, *Adv. Mater.*, 2006, **18**, 973–989.
29 O. Pitois and B. François, *Colloid Polym. Sci.*, 1999, **277**, 574–578.
30 H. Yabu, M. Tanaka, K. Ijiro and M. Shimomura, *Langmuir*, 2003, **19**, 6297–6300.
31 L. Song, R. K. Bly, J. N. Wilson, S. Bakbak, J. O. Park, M. Srinivasarao and U. H. F. Bunz, *Adv. Mater.*, 2004, **16**, 115–118.
32 T. Nishikawa, M. Nonomura, K. Arai, J. Hayashi, T. Sawadaishi, Y. Nishiura, M. Hara and M. Shimomura, *Langmuir*, 2003, **19**, 6193–6201.
33 A. Böker, Y. Lin, K. Chiapperini, R. Horowitz, M. Thompson, V. Carreon, T. Xu, C. Abetz, H. Skaff, A. D. Dinsmore, T. Emrick and T. P. Russell, *Nat. Mater.*, 2004, **3**, 302–306.
34 K. H. Wong, M. Hernández-Guerrero, A. M. Granville, T. P. Davis, C. Barner-Kowollik and M. H. Stenzel, *J. Porous Mater.*, 2006, **13**, 213–223.
35 T. Nishikawa, R. Ookura, J. Nishida, K. Arai, J. Hayshi, N. Kurono, T. Sawadaishi, M. Hara and M. Shimomura, *Langmuir*, 2002, **18**, 5734–5740.
36 L. A. Connal, P. A. Gurr, G. G. Qiao and H. D. Solomon, *J. Mater. Chem.*, 2005, **15**, 1286–1292.
37 V. L. Govor, I. A. Bashmakov, R. Kiebooms, V. Dyakonov and J. Parisi, *Adv. Mater.*, 2001, **13**, 588–591.
38 S. D. Angus and T. P. Davis, *Langmuir*, 2002, **18**, 9547–9553.
39 X. Zhao, Q. Cai, G. Shi, Y. Shi and G. Chen, *J. Appl. Polym. Sci.*, 2003, **90**, 1846–1850.
40 W. Kasai and T. Kondo, *Macromol. Biosci.*, 2004, **4**, 17–21.
41 T. H. Ham, I. J. Chung, Y. S. Choi, S. H. Lee and S. O. Kim, *J. Phys. Chem. B*, 2006, **110**, 13959–13964.
42 Y. Wang, Z. Liu, Y. Huang, B. Han and G. Yan, *Langmuir*, 2006, **22**, 1928–1931.
43 M. S. Park and J. K. Kim, *Langmuir*, 2004, **205**, 5347–5352.
44 W. Sun, Z. Shao and J. A. Ji, *Polymer*, 2010, **51**, 4169–4175.
45 C. J. Lawrence, *Phys. Fluids*, 1988, **31**, 2786–2796.
46 A. J. Hurd, *Evaporation and Surface Tension Effects in Dip Coating*, Advances in Chemistry, ACS, 1994, vol. 234, ch. 21, pp. 433–450.
47 E. Bormashenko, R. Pogreb, O. Stanevsky, Y. Bormashenko, T. Stein, V.-Z. Gaisin, R. Cohen and O. V. Gendelman, *Macromol. Mater. Eng.*, 2005, **290**, 114–121.
48 M. Orlov, I. Tokarev, A. Scholl, A. Doran and S. Minko, *Macromolecules*, 2007, **40**, 2086–2091.
49 W. Madej, A. Budkowski, J. Raczkowska and J. Rysz, *Langmuir*, 2008, **24**, 3517–3524.
50 M. S. Park and J. K. Kim, *Langmuir*, 2005, **21**, 11404–11408.
51 M. S. Park, W. Joo and J. K. Kim, *Langmuir*, 2006, **22**, 4594–4598.
52 F. Pilati, M. Montecchi, P. Fabbri, A. Synytska, M. Messori, M. Toselli, K. Grundke and D. Pospiech, *J. Colloid Interface Sci.*, 2007, **315**, 210–222.
53 A. Munoz-Bonilla, E. Ibarboure, E. Papon and J. Rodriguez-Hernandez, *J. Polym. Sci., Part A: Polym. Chem.*, 2009, **47**, 2262–2271.
54 K. I. Hiwatari, T. Serizawa, F. Seto, A. Kishida, Y. Muraoka and M. Akashi, *Polym. J.*, 2001, **33**, 669–675.
55 M. H. Stenzel, *Aust. J. Chem.*, 2002, **55**, 239–243.
56 N. Maruyama, O. Karthaus, K. Ijiro, M. Shimomura, T. Koito, S. Nishimura, T. Sawadaishi, N. Nishi and S. Tokura, *Supramol. Sci.*, 1998, 331–336.
57 J. Peng, Y. Han, J. Fu, Y. Yang and B. Li, *Macromol. Chem. Phys.*, 2003, **204**, 125–1130.
58 N. Maruyama, T. Koito, J. Nishida, T. Sawadaishi, X. Cieren, K. Ijiro, O. Karthaus and M. Shimomura, *Thin Solid Films*, 1998, **327–329**, 854–856.
59 K. H. Wong, T. P. Davis, C. Barner-Kowollik and M. H. Stenzel, *Polymer*, 2007, **48**, 4950–4965.
60 Y. Wang, Z. Liu, B. Han, H. Gao, J. Zhang and X. Kuang, *Chem. Commun.*, 2004, (7), 800–801.
61 C. L. Lin, P.-H. Tung and F.-C. Chang, *Polymer*, 2005, **46**, 9304–9313.
62 C. Yu, J. Zhai, X. Gao, M. Wan, L. Jian, T. Li and Z. Li, *J. Phys. Chem. B*, 2004, **108**, 4586–4589.
63 W. Bu, H. Li, H. Sun, S. Yin and L. Wu, *J. Am. Chem. Soc.*, 2005, **127**, 8016–8017.
64 J. S. Park, S. H. Lee, T. H. Han and S. O. Kim, *Adv. Funct. Mater.*, 2007, **17**, 2315–2320.
65 J. Li, J. Peng, W. Huang, Y. Wu, J. Fu, Y. Cong, L. Xue and Y. Han, *Langmuir*, 2005, **21**, 2017–2021.
66 S. Sakurai, C. Furukawa, A. Okutsu, A. Miyoshi and S. Nomura, *Polymer*, 2002, **43**, 3359–3364.
67 G. D. Fu, E. T. Kang and K. G. Neoh, *Langmuir*, 2005, **21**, 3619–3624.
68 S. X. Wang, M. T. Wang, Y. Lei and L. D. Zhang, *Mater. Res. Bull.*, 2000, **35**, 1625–1630.
69 A. E. Saunders, J. L. Dickson, P. S. Shah, M. Y. Lee, K. Lim, K. P. Johnston and B. A. Korgel, *Phys. Rev. E: Stat., Nonlinear, Soft Matter Phys.*, 2006, **73**, 031608.

70 Y. Tian, H. Ding, Q. Jiao and Y. Shi, *Macromol. Chem. Phys.*, 2006, **207**, 545–553.

71 L. Billon, M. Manguian, V. Pellerin, M. Joubert, O. Eterradossi and H. Garay, *Macromolecules*, 2009, **42**, 345–356.

72 Y. Tian, C. Dai, H. Ding, Q. Jiao, L. Wang, Y. Shi and B. Liu, *Polym. Int.*, 2007, **56**, 834–839.

73 C. Cheng, Y. Tian, Y. Shi, R. Tang and F. Xi, *Macromol. Rapid Commun.*, 2005, **26**, 1266–1272.

74 B. Zhao, J. Zhang, H. Wu, X. Wang and C. Li, *Thin Solid Films*, 2007, **515**, 3629–3634.

75 J. Li, J. T. Cheng, Y. Zhang and P. Gopalakrishnakone, *Colloid Polym. Sci.*, 2009, **287**, 29–36.

76 B. M. H. Nurmawati, M. Vetrichelvan and S. Valiyaveettil, *J. Porous Mater.*, 2006, **13**, 315–317.

77 C. Wang, Q. Liu, X. Shao, G. Yang, H. Xue and X. Hu, *Talanta*, 2007, **71**, 178–185.

78 L. A. Connal and G. G. Qiao, *Adv. Mater.*, 2006, **18**, 3024–3028.

79 L. A. Connal and G. G. Quiao, *Soft Matter*, 2007, **3**, 837–839.

80 P. Escale, S. R. S. Ting, A. Khoukh, L. Rubatat, M. Save, M. H. Stenzel and L. Billon, *Macromolecules*, 2011, **44**, 5911–5919.

81 J.-S. Wang and K. Matyjaszewski, *J. Am. Chem. Soc.*, 1995, **117**, 5614–5615.

82 K. Karaky, L. Billon, C. Pouchan and J. Desbrières, *Macromolecules*, 2007, **40**, 458–464.

83 K. Karaky, G. Clisson, G. Reiter and L. Billon, *Macromol. Chem. Phys.*, 2008, **209**, 715–722.

84 J. Chiefari, Y. K. Chong, F. Ercole, J. Krstina, J. Jeffrey, T. P. T. Le, R. T. A. Mayadune, G. F. Meijs, C. Moad, G. Moad, E. Rizzardo and S. H. Thang, *Macromolecules*, 1998, **31**, 5559–5562.

85 C. Barner-Kowollik, T. P. Davis, J. P. A. Heuts, M. H. Stenzel, P. Vana and M. Whittaker, *J. Polym. Sci., Part A: Polym. Chem.*, 2003, **41**, 365–375.

86 M. H. Stenzel and T. P. Davis, *J. Polym. Sci., Part A: Polym. Chem.*, 2002, **40**, 4498–4512.

87 M. Hernandez-Guerrero, T. P. Davis, C. Barner-Kowollik and M. H. Stenzel, *Eur. Polym. J.*, 2005, **41**, 2264–2277.

88 M. H. Stenzel-Rosenbaum, T. P. Davis, A. G. Fane and V. Chen, *Angew. Chem., Int. Ed.*, 2001, **40**, 3428–3432.

89 M. H. Stenzel-Rosenbaum and T. P. Davis, PCT/AU01/01639, 2002.

90 M. H. Stenzel, C. Barner-Kowollik and T. P. Davis, *J. Polym. Sci., Part A: Polym. Chem.*, 2006, **44**, 2363–2375.

91 W. Y. Dong, Y. F. Zhou, D. Y. Yan, Y. Y. Mai, L. He and C. Y. Jin, *Langmuir*, 2009, **25**, 173–178.

92 C. Xia, Y. Tian, Y. Qiao Shi, R. Pei Tang and F. Xi, *Langmuir*, 2005, **21**, 6576–6581.

93 B. François, Y. Ederlé and C. Mathis, *Synth. Met.*, 1999, **103**, 2362–2363.

94 M. H. Stenzel, T. P. Davis and A. G. Fane, *J. Mater. Chem.*, 2003, **13**, 2090–2097.

95 J. Peng, Y. Han, Y. Yang and B. Li, *Polymer*, 2004, **45**, 447–452.

96 L. Cui, J. Peng, Y. Ding, X. Li and H. Han, *Polymer*, 2005, **46**, 5334–5340.

97 A. Bolognesi, C. Mercogliano, S. Yunus, M. Civardi, D. Comoretto and A. Turturro, *Langmuir*, 2005, **21**, 3480–3485.

98 M. H. Stenzel and T. P. Davis, *Aust. J. Chem.*, 2003, **56**, 1035–1038.

99 A. Nygard, T. P. Davis, C. Barner-Kowollik and M. H. Stenzel, *Aust. J. Chem.*, 2005, **58**, 595–599.

100 B. De Boer, U. Stalmach, H. Nijland and G. Hadziioannou, *Adv. Mater.*, 2000, **12**, 1581–1583.

101 X. J. Hao, M. H. Stenzel, C. Barner-Kowollik, T. P. Davis and E. Evans, *Polymer*, 2004, **45**, 7401–7415.

102 T. Hayakawa and S. Horiuchi, *Angew. Chem., Int. Ed.*, 2003, **42**, 2285–2289.

103 J. Li, Q. L. Zhao, J. Z. Chan, L. Li, J. Huang, Z. Ma and Y. W. Zhong, *Polym. Chem.*, 2010, **1**, 164–167.

104 B. S. Kim, C. Basavaraja, E. Jo, D. G. Kim and D. S. Huh, *Polymer*, 2010, **51**, 3365–3371.

105 H. M. Dalton, J. Stein and P. E. March, *Biofouling*, 2000, **15**, 83–94.

106 H. M. Dalton and M. H. Stenzel, Centre for Advanced Macromolecular Design, Sydney, Australia, 2005, unpublished results.

107 P. Escale, M. Save, A. Lapp, L. Rubatat and L. Billon, *Soft Matter*, 2010, **6**, 3202–3210.

108 B. B. Ke, L. S. Wan, W. X. Zhang and Z. K. Xu, *Polymer*, 2010, **51**, 2168–2176.

109 Y. Fukuhira, H. Yabu, K. Ijiro and M. Shimomura, *Soft Matter*, 2009, **5**, 2037–2041.

110 M. Kojima, Y. Hirai, H. Yabu and M. Shimomura, *Polym. J.*, 2009, **41**, 667–671.

111 B. S. Kim, C. Basavaraja, E. A. Jo, D. G. Kim and D. S. Huh, *Polymer*, 2010, **51**, 3365–3371.

112 Y. Maeda, Y. Shimoi and K. Ogino, *Polym. Bull.*, 2005, **53**, 315–321.

113 S. M. Hant, G. S. Attar, R. Riddle and K. M. Ryan, *Chem. Mater.*, 2005, **17**, 1434–1440.

114 M. Pintani, J. Huang, M. C. Ramon and D. D. C. Bradley, *J. Phys.: Condens. Matter*, 2007, **19**, 016203.

115 H. Takamori, T. Fujigaya, Y. Yamaguchi and N. Nakashima, *Adv. Mater.*, 2007, **19**, 2535–2539.

116 C. Liu, C. Gao and D. Yan, *Angew. Chem., Int. Ed.*, 2007, **46**, 4128–4131.

117 D. Fan, X. Jia, P. Tang, J. Hao and T. Liu, *Angew. Chem., Int. Ed.*, 2007, **46**, 3342–3345.

118 M. Srinivasarao, D. Collings, A. Philips and S. Patel, *Science*, 2001, **292**, 79–83.

119 Y. Xu, B. Zhu and Y. Xu, *Polymer*, 2005, **46**, 713–717.

120 H. Yabu, M. Kojima, M. Tsubouchi, S. Onoue, M. Sutitani and M. Shimomura, *Colloids Surf., A*, 2006, **284–285**, 254–256.

121 A. S. Karikari, S. R. Williams, C. L. Heisey, A. M. Rawlett and T. E. Long, *Langmuir*, 2006, **22**, 9687–9693.

122 L. Li, Y. W. Zhong, J. Li, C. K. Chan, A. J. Zhang, J. Xu and Z. Ma, *J. Mater. Chem.*, 2009, **19**, 7222–7227.

123 L. Li, C. K. Chen, A. J. Zhang, X. Y. Liu, K. Cui, J. Huang, Z. Ma and Z. H. Han, *J. Colloid Interface Sci.*, 2009, **331**, 446–452.

124 F. Galeotti, V. Calabrese, M. Cavazzini, S. Quici, C. Poleunis, S. Yunus and A. Bolognesi, *Chem. Mater.*, 2010, **22**, 2764–2769.

125 H. Sun, H. L. Li and L. X. Wu, *Polymer*, 2009, **50**, 2113–2122.

126 S. R. S. Ting, E. H. Min, P. Escale, M. Save, L. Billon and M. H. Stenzel, *Macromolecules*, 2009, **42**, 9422–9434.

127 A. Munoz-Bonilla, E. Ibarboure, V. Bordege, M. Fernandez-Garcia and J. Rodriguez-Hernandez, *Langmuir*, 2010, **26**, 8552–8558.

128 E. H. Min, S. R. S. Ting, L. Billon and M. H. Stenzel, *J. Polym. Sci., Part A: Polym. Chem.*, 2010, **48**, 3440–3455.

129 B. B. Ke, L. S. Wan and Z. K. Xu, *Langmuir*, 2010, **26**, 8946–8952.

130 D. Nystrom, E. Malmstrom, A. Hult, I. Blakey, C. Boyer, T. P. Davis and M. R. Whittaker, *Langmuir*, 2010, **26**, 12748–12754.

131 E. H. Min, K. H. Wong and M. H. Stenzel, *Adv. Mater.*, 2008, **20**, 3350–3556.

132 A. Munoz-Bonilla, E. Ibarboure, E. Papon and J. Rodriguez-Hernandez, *Langmuir*, 2009, **25**, 6493–6499.

133 A. Bolognesi, F. Galeotti, J. Moreau, U. Giovanella, W. Porzio, G. Scavia and F. Bertini, *J. Mater. Chem.*, 2010, **20**, 1483–1488.

134 L. Cui, Y. Xuan, X. Li, Y. Ding, B. Li and Y. Han, *Langmuir*, 2005, **21**, 11696–11703.

135 Y. Uraki, C. Matsumoto, T. Hirai, Y. Tamai, M. Enoki, H. Yabu, M. Tanaka and M. Shimomura, *J. Wood Chem. Technol.*, 2010, **30**, 348–359.

136 C. Barner-Kowollik, H. Dalton, T. P. Davis and M. H. Stenzel, *Angew. Chem., Int. Ed.*, 2003, **115**, 3792–3796.

137 M. L. K. Hoa, M. Lu and Y. Zhang, *Adv. Colloid Interface Sci.*, 2006, **121**, 9–23.

138 T. Nishikawa, J. Nishida, R. Ookura, S.-I. Nishimura, S. Wada, T. Karino and M. Shimomura, *Mater. Sci. Eng., C*, 1999, **10**, 141–146.

139 L. Ghanam, H. Garay, J. François and L. Billon, *Macromol. Chem. Phys.*, 2007, **208**, 1469–1479.

140 L. Ghanam, M. Manguian, J. François and L. Billon, *Soft Matter*, 2007, **3**, 1492–1499.

141 L. Heng, Z. Zhai, Y. Zhao, J. Xu, X. Sheng and L. Jiang, *ChemPhysChem*, 2006, **7**, 2520–2525.

142 A. Bolognesi, C. Botta and S. Yunus, *Thin Solid Films*, 2005, **492**, 307–312.

143 H. Yabu, K. Akagi and M. Shimomura, *Synth. Met.*, 2009, **159**, 762–764.

144 K. H. Wong, M. H. Stenzel, S. Duvall and F. Ladouceur, *Chem. Mater.*, 2010, **22**, 1878–1891.

145 H. Yabu, Y. Hirai and M. Shimomura, *Langmuir*, 2006, **22**, 9760–9764.

146 D. Ishii, H. Yabu and M. Shimomura, *Colloids Surf., A*, 2008, **313–314**, 590–594.

147 Y. Hirai, H. Yabu and M. Shimomura, *Colloids Surf., A*, 2008, **313–314**, 312–315.

148 T. Ohzono and M. Shimomura, *Colloids Surf., A*, 2006, **284–285**, 505–508.

149 F. Galeotti, I. Chiusa, L. Morello, S. Giani, D. Braviano, S. Hatz, F. Damin, M. Chiari and A. Bolognesi, *Eur. Polym. J.*, 2009, **45**, 3027–3034.

150 L. Li, Y. W. Xhong, J. Li, J. L. Gong, Y. Ben, J. Xu, X. P. Chen and Z. Ma, *J. Colloid Interface Sci.*, 2010, **342**, 192–197.

151 Y. Hirai, H. Yabu, Y. Matsuo, K. Ijiro and M. Shimomura, *J. Mater. Chem.*, 2010, **20**, 10804–10808.

152 H. M. Ma and J. C. Hao, *Chem.–Eur. J.*, 2010, **16**, 655–660.

153 H. Hirai, H. Yabu, Y. Matsuo, K. Ijiro and M. Shimomura, *Chem. Commun.*, 2010, **46**, 2298–2300.

154 H. Sunami, E. Ito, M. Tanaka, S. Yamamoto and M. Shimomura, *Colloids Surf., A*, 2006, **284–285**, 548–551.

155 D. Beattie, K. H. Wong, C. Williams, L. A. Poole-Warren, T. P. Davis, C. Barner-Kowollik and M. H. Stenzel, *Biomacromolecules*, 2006, **7**, 1072–1082.

156 M. Tanaka, A. Takayama, E. Ito, H. Sunami, S. Yamamoto and M. Shimomura, *J. Nanosci. Nanotechnol.*, 2007, **7**, 763–722.

157 M. Tanaka, K. Yoshizawa, A. Tsuruma and H. Sunami, *Colloids Surf., A*, 2008, **313–314**, 515–519.

158 M. Hernandez-Guerrero, E. Min, C. Barner-Kowollik, A. H. E. Müller and M. H. Stenzel, *J. Mater. Chem.*, 2008, **18**, 4718–4730.

159 S. Tsukiyama, M. Matsushita, M. Tanaka, H. Tamura, S. Todo, S. Yamamoto and M. Shimomura, *Jpn. J. Appl. Phys.*, 2008, **47**, 1429–1434.

160 L. Li, C. K. Chen, A. J. Zhang, X. Y. Liu, B. Xu, S. B. Gao, G. H. Jin and Z. Ma, *J. Mater. Chem.*, 2009, **19**, 2789–2796.

161 Y. Fukuhira, M. Ito, H. Kaneko, Y. Sumi, M. Tanaka, S. Yamamoto and M. Shimomura, *J. Biomed. Mater. Res., Part B*, 2008, **86**, 353–359.

162 T. Okuda, T. Higashide, Y. Fukuhira, Y. Sumi, M. Shimomura and S. Kazuhisa, *J. Glaucoma*, 2009, **18**, 220–226.

163 J. Bico, C. Marzolin and D. Quéré, *Europhys. Lett.*, 1999, **47**, 220–226.

164 H. Yabu, M. Takebayashi, M. Tanaka and M. Shimomura, *Langmuir*, 2005, **21**, 3235–3237.

165 H. Yabu and M. Shimomura, *Chem. Mater.*, 2005, **17**, 5231–5234.

166 S. I. Matsushita, N. Kurono, T. Sawadaishi and M. Shimomura, *Synth. Met.*, 2004, **147**, 237–240.

167 M. H. Lu and Y. Zhang, *Adv. Mater.*, 2006, **18**, 3094–3098.

168 X. L. Jiang, X. F. Zhou, Y. Zhang, T. Z. Zhang, Z. R. Guo and N. Gu, *Langmuir*, 2010, **26**, 2477–2438.

169 L. S. Wan, B. B. Ke, X. K. Li, X. L. Meng, L. Y. Zhang and Z. K. Xu, *Sci. China, Ser. B: Chem.*, 2009, **52**, 969–974.

170 H. Sun, W. Li and L. X. Wu, *Langmuir*, 2009, **25**, 10466–10472.

171 L. A. Connal, G. V. Franks and G. G. Qiao, *Langmuir*, 2010, **26**, 10397.